ISSN 0208-7774 TRIBOLOGIA 4/2018 p. 63–69

Jerzy NAPIÓRKOWSKI[*], Łukasz KONAT[**], Marta PIETRUSZEWSKA[*]

EFFECT OF LASER HARDENING OF STEEL ON THE WEAR PROCESS IN AN ABRASIVE SOIL MASS

WPŁYW HARTOWANIA LASEROWEGO STALI NA PROCES ZUŻYWANIA W GLEBOWEJ MASIE ŚCIERNEJ

Key words: laser hardening, wear intensity, soil mass.

Abstract This paper presents the results of tests for the effects of laser hardening on the course and intensity of wear of 38GSA (38MnSi4) and Hardox 600 steels in an abrasive soil mass. The tests were carried out under laboratory conditions, using a "rotating bowl" type machine. Two types of soil, i.e. light and medium, were used as the abrasive mass. Based on the obtained test results, it was found that hardness decreased (in relation to as-delivered condition). The performed laser surface hardening process significantly increased the abrasive wear resistance only for 38GSA (38MnSi4) steel. As regards to Hardox steel, the hardening treatment reduced the abrasive wear resistance index compared to the as-delivered condition of the steel.

Słowa kluczowe: hartowanie laserowe, intensywność zużycia, masa glebowa.

Streszczenie W pracy przedstawiono wyniki badań wpływu hartowania laserowego na przebieg i intensywność zużywania stali 38GSA (38MnSi4) i Hardox 600 w glebowej masie ściernej. Badania przeprowadzono w warunkach laboratoryjnych, wykorzystując maszynę typu „wirująca misa". Masę ścierną stanowiły dwa rodzaje gleby: lekka i średnia. Na podstawie uzyskanych wyników badań stwierdzono, że twardość uległa zmniejszeniu (w stosunku do stanu dostarczenia). Przeprowadzenie procesu hartowania powierzchniowego laserem spowodowało wyraźne podwyższenie odporności na zużywanie ścierne jedynie stali 38GSA (38MnSi4). W odniesieniu do stali Hardox zabieg hartowania spowodował zmniejszenie wskaźnika odporności na zużywanie ścierne w stosunku do stanu dostarczenia tej stali.

INTRODUCTION

The durability of operating parts working within a soil mass, *inter alia* in mining, agriculture, and road construction, is among the lowest of all machinery functional units. The wear in an abrasive soil mass has so far been the least researched of all abrasive wear processes. All studies **[L. 1–3]** mention the following, *inter alia*, as major factors determining the course of wear of materials: hardness and deformability of operating parts, chemical composition, and microstructure of an operating part, as well as acidity, compactness, grain-size distribution and moisture content of a soil mass, the size and shape of abrasive grains, and the number of actively operating grains. It was found, among other things, that grain-size distribution of soil is a summary of the characteristics of determined physical properties of the soil and is a basic parameter describing its wear impact. Increasing operating speed, unit pressure, and dynamic loads also increase the risk of quicker wear.

Hence, new technologies for the production of these materials are being developed with the aim of slowing down the process of their operational wear. These measures are taken in two directions. On the one hand, new construction materials, such as highly resistant, low-alloyed steels described as materials resistant to abrasive wear are being developed. On the other hand, multi-layered padding welds based on transition metals and amphoteric elements, applied onto surfaces subjected to the most intensive wear **[L. 4]** are being developed as well. The basic properties of these materials should be aimed at high resistance to abrasive wear, the ability

[*] University of Warmia and Mazury in Olsztyn, ul. Michała Oczapowskiego 2, 10-719 Olsztyn, Poland, e-mail: napj@uwm.edu.pl.
[**] Wrocław University of Technology, Wybrzeże Wyspiańskiego 27, 50-370 Wrocław, Poland, e-mail: lukasz.konat@pwr.edu.pl.

to transmit heavy loads of a random nature, and the homogeneity of properties over the entire section of an operating part. These properties are achievable through obtaining a homogeneous structure of these steels over the entire section of structural components made of them. In turn, the possibility for obtaining homogeneous structures over large sections is dictated by the very precise selection of the chemical composition as a function of sheet thickness, the presence of boron micro-addition, a reduced content of harmful impurities, and specialised heat treatment or heat and plastic forming measures. Due to high usefulness, in most cases, they are still the basic construction material used to produce operating parts of tools and selected parts of machinery. This results, on the one hand, from the advantageous relationship of the costs of their manufacture and, on the other, from their versatility.

Laser technologies are increasingly being applied in the production of construction materials **[L. 5]**. Laser welding, pad-welding, and heat treatment technologies have many advantages that make them superior to conventional technologies. As regards to hardening, these include the following: the possibility of obtaining a finer martensitic structure with increased hardness, the possibility of selective hardening of a selected surface with an increased carbon content, and the lack of thermal deformations. An unambiguous assessment of suitability of the group of materials concerned for the selected area of application is very difficult and requires a complex, comprehensive approach to this issue. According to the authors of this paper, the starting point for such an assessment is structural and tribological studies. Therefore, the aim of the study is to analyse the effects of laser-hardened layers on the process of steel wear under varying soil conditions.

RESEARCH MATERIAL AND METHODS

For the study, two grades of steel characterised as resistant to abrasive wear, namely 38GSA (38MnSi4) and Hardox 600, were selected. Results of research concerning the processes of abrasive wear in an abrasive soil mass are repeatedly referred to the 38GSA (38MnSi4) grade steel developed as a special purpose material. Sheets of this steel, from which test material was collected, were manufactured using hot rolling technology and were subjected to heat refining. In Poland, 38GSA (38MnSi4) steel is most commonly used to manufacture operating parts in the agricultural sector. On the other hand, Hardox 600 steel samples were collected from 10 mm thick sheets supplied by the distributor of the steel in a hardened condition. According to the producer's data **[L. 6]**, Hardox steels are supplied as water-hardened and tempered at a temperature of 200–700°C, which ensures obtaining a homogeneous hardness over 90% of the section of sheet, which amounts to 550–640 HBW. Hardox 600 steel is most commonly used in the form of metal sheets with a thickness of 6-65 mm. In addition, this steel can be subjected to welding processes, provided that it is preceded by initial preheating. In order to maintain high hardness in a hardened condition, preheating of sheets made of this steel to a temperature over 200°C is not recommended. Samples of the tested steels were collected in the form of rectangles with dimensions of 30×25×10 mm using methods ensuring the stability of their structure. Five samples were prepared for each of the test variants. The samples were cut out using the high-energy abrasive water jet method.

Tests for resistance to abrasive wear were conducted in accordance with the "rotating bowl" method using a MZWM–1 device. The general structure and a diagram of the device are shown in **Fig. 1**.

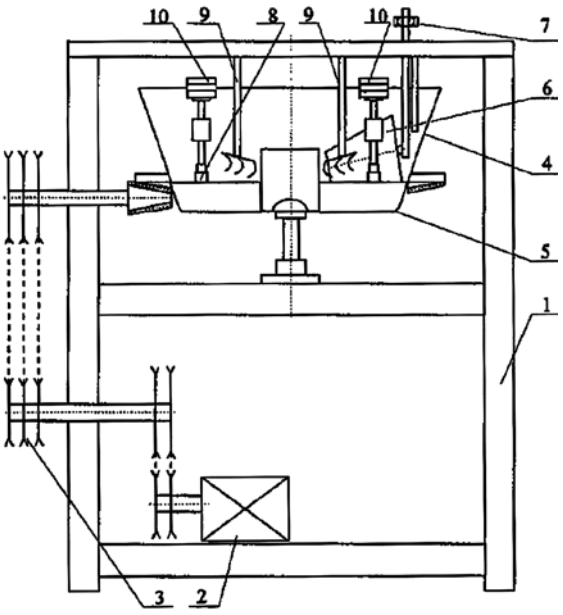

Fig. 1. A stand for testing wear in an abrasive soil mass: 1 – frame, 2 – motor, 3 – belt transmission, 4 – bowl, 5 – soil, 6 – pressing rolls, 7 – roll clamp, 8 – holder with a sample, 9 – loosening fork, 10 – sample weights

Rys. 1. Stanowisko do badania zużycia w glebowej masie ściernej: 1 – rama, 2 – silnik, 3 – przekładnia pasowa, 4 – misa, 5 – gleba, 6 – rolki ugniatające, 7 – docisk rolki, 8 – uchwyt z próbką, 9 – widełki spulchniające, 10 – obciążniki próbki

The machine rests on a self-supporting frame to which operating units are attached. Test samples are fixed on two independent sections mounted on an independent balance level suspension. The core of the balance lever was equipped with a special pin enabling the use of sample ballast weights. In order to eliminate initial stresses, the abrasive mass was loosened and levelled by two loosening mechanisms. Grain-size distribution of soil, determined using a Mastersizer 2000 laser particle size analyser, is provided in **Table 1**.

Table 1. Characteristics of the abrasive soil mass (Polish Soil Science Society (PTG) classification, 2008)
Tabela 1. Charakterystyka glebowej masy ściernej (klasyfikacja PTG 2008)

Soil mass type	Granulometric group	Fraction content [%]			Moisture content by weight [%]
		Sand 2.00-0.05 mm	Silt 0.050-0.002 mm	Clay < 0.002 mm	
LIGHT	Loamy sand	77.48	20.83	1.69	9-11
HEAVY	Common loam	33.62	49.92	16.56	12-14

During the testing, the following friction parameters were adopted: a velocity of 1.66 m/s, a friction distance of 20 000 m, and a unit pressure of 67 kPa. The mass wear was measured every 2000 m. During the tests, a slightly acidic pH value of the soil of 6.4–6.8 was provided. The pH values were measured according to the electrometric method using an EpH-117/118 meter manufactured by Alsmeer-Holland. The moisture content of the soil was determined using the oven-drying method through a measurement of the weight of the dried solid phase at a temperature of 105 °C, according to Formula (1):

$$W = \frac{m_1 - m_2}{m_2 - m_n} \times 100\% \quad (1)$$

where: W – moisture content [%],
m_1 – soil sample weight prior to drying [g],
m_2 – sample weight after drying [g],
m_n – sample container weight [g].

Sample weight loss was measured on laboratory scales with an accuracy of 0.0001 g. Prior to testing, samples were subjected to precision grinding to ensure a roughness of Ra = 0.22-0.28 μm along the friction plane, and Ra = 0.32-0.42 μm in the perpendicular plane. Each measurement of the weight was preceded by cleaning a sample in an ultrasonic cleaner. The mass wear was determined using Formula (2):

$$Z_{pw} = m_w - m_i \quad (2)$$

where: Z_{pw} – sample weight loss after the pre-determined friction distance s [g],
m_w – initial sample weight prior to friction test [g],
m_i – sample weight after covering the friction distance s [g].

Analyses of chemical compositions were carried out in accordance with the spectral method using a GDS500A Glow Discharge Atomic Emission Spectrometer manufactured by Leco. During the analyses, the following parameters were applied: U = 1250 V, I = 45 mA, 99.999% argon. The obtained results were an arithmetic mean of at least five measurements.

Microstructure observations were conducted using a Nikon Eclipse MA200 optical microscope coupled with a Nikon DS-Fi2 digital camera, using NIS Elements software. Light microscopy observations were conducted at magnifications within the range of 100-1000x.

Measurements of hardness using the Brinell hardness test method were performed in accordance with standard PN-EN ISO 6506-1:2014-12 with a Zwick ZHU hardness tester with a 2.5 mm sintered carbide ball, with a load of 1 875 N operating for 15 s. Measurements of hardness using the Vickers method were carried out in accordance with the procedure provided in standard PN-EN ISO 6507-1:2007. They were conducted using a Mitutoyo MMT-X7B hardness tester with a load of 9.81 N operating for 15 s. All measurements were carried out on samples subjected to a previous assessment of the microstructure on cross-sections of sheets.

Laser hardening was carried out using a 6 kW Nd:YAG diode fibre-optic laser (**Fig. 2**). It allowed the beam to be directed to hard-to-reach places while ensuring full precision of the beam advance. A robot is located on a compound rotary table with a load capacity of 500–2000 kg, a tilting axis of 140°, and an axis of rotation of 360°. The system of laser power control was operated automatically using a thermal camera monitoring the temperature of material surface. The hardening parameters are presented in **Table 2**. They were selected experimentally as part of a parallel research experiment. The value of welding energy was determined algebraically from Formula (3), taking account of the applied welding parameters. The value of laser radiation energy efficiency index η was assumed to be equal to 0.2, in accordance with the data presented in paper **[L. 7]**.

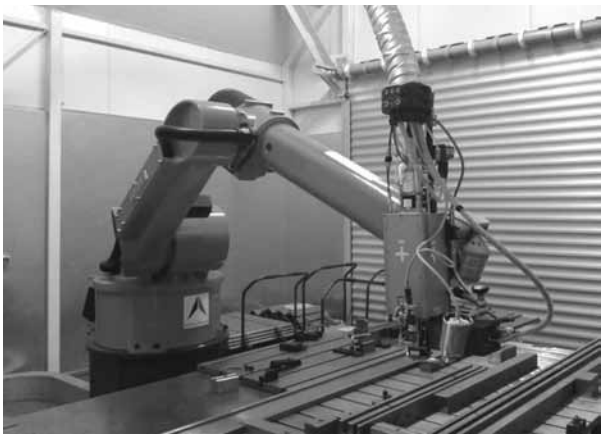

Fig. 2. A robot controlling a laser-hardening head
Rys. 2. Robot sterujący głowicą hartującą laserowo

$$Q = \eta \cdot \frac{P}{v} \quad (3)$$

where: Q – welding energy [J/mm],
P – laser radiation power [W],
ν – welding rate [mm/s],
η – laser radiation energy efficiency index [-].

Table 2. Basic parameters of hardening of 38GSA (38MnSi4) and Hardox 600 steels samples
Tabela 2. Podstawowe parametry hartowania próbek stali 38GSA (38MnSi4) i stali Hardox 600

Item	Steel	Hardening parameters	Welding energy
1	38GSA (38MnSi4)	1250 °C; 6 mm/s; 2950 W	93 J/mm
2	Hardox 600	1250 °C; 6 mm/s; 2400 W	80 J/mm

STUDY RESULTS

Table 3 presents the results of conducted spectral analyses of chemical composition, and selected mechanical properties of the steels under study. Having excluded 38GSA (38MnSi4) steel from considerations, as it has already been a subject of studies in this regard, as reported by the authors in previous papers **[L. 2–3]**, it can be generally concluded that for, the sheet thickness concerned (10 mm), the actual quantities of alloy additions in Hardox 600 steel significantly deviate from maximum values provided by the producer. The only exception is carbon content (0.41%), which was close to the declared upper limit for this element. In addition, the presence of chemical elements not mentioned in the material issue list was found in the chemical composition of Hardox 600 steel. These elements include, *inter alia*, copper, aluminium, titanium, and cobalt. It can therefore be concluded that, for Hardox 600 steel, there is no possibility for its classification based on chemical composition, according to the international standard. However, it needs to be indicated that chemical composition of Hardox steel is selected with the aim of obtaining the assumed level of hardness and the carbon equivalent CEV. Therefore, the chemical composition of these steels changes as a function of sheet thickness.

In general, it can be concluded that carbide-forming elements such as Cr, Mo, and Ti retard diffusional transformations by increasing hardenability. Chromium and molybdenum are very frequently used in combination due to the chromium's tendency to increase the susceptibility to steel brittleness during tempering processes. Micro-additions of aluminium and titanium bind nitrogen and prevent the growth of grains during austenitising prior to heat treatment measures. On the other hand, nickel is added to decrease the temperature of austenitising, and to decrease the temperature of the ductile to brittle transition.

Table 3. Chemical compositions and selected mechanical properties of tested steels [L. 2, 6, 8, 9]
Tabela 3. Składy chemiczne i wybrane właściwości mechaniczne badanych stali **[L. 2, 6, 8, 9]**

Chemical element [% w/w]	38GSA (38MnSi4)		Hardox 600	
	OR – based on own research; PD – producer's data			
	OR[1]	PD[2]	OR[3]	PD[3]
C	0.38	0.34-0.42	0.41	≤ 0.45
Mn	0.97	0.70-1.10	0.51	≤ 1.00
Si	0.90	0.80-1.10	0.14	≤ 0.70
P	0.011	≤ 0.035	0.006	≤ 0.015
S	0.007	≤ 0.040	0.001	≤ 0.010
Cr	0.05	≤ 0.30	0.32	≤ 1.20
Ni	0.08	≤ 0.30	1.96	≤ 2.50
Mo	0.02	-	0.14	≤ 0.80
Cu	0.25	≤ 0.30	0.02	-
Al	0.02	0.02-0.06*	0.04	-
Ti	0.002	0.03-0.06*	0.003	-
Co	0.01	-	0.017	-
B	-	-	0.0017	≤ 0.004
HBW (HV)	272 ±7 (286)	440	549 ±6 (584)	550-640
R_e [MPa]	-	1200	-	1650
R_e [MPa]	-	1500	-	2000
A_5 [%]	-	8	-	12
KCV_{-40} [J/cm^2]	-	30**	-	25

[1] condition after standardisation; [2] condition after hardening (870–900°C/water) and tempering (200–250°C in the air or in oil); [3] in an as-delivered condition; *if combined, then Al+Ti ≥ 0.03% w/w.; **KCU_{+20}

Figures 3–7 present representative microstructures of the tested steels, both in an as-delivered condition and after laser hardening treatment. In an as-delivered condition (standardised condition), 38GSA (38MnSi4) steel is characterised by a fine-grained ferrite-pearlite structure (**Figs. 3a** and **4a)**. On the other hand, the microstructure of Hardox 600 steel in a condition analogous to that of 38GSA (38MnSi4) steel (**Figs. 3b** and **4b**) comprises hardened martensite with a fine-stripped structure and with areas of tampered martensite. Inside the martensite strips, very few carbide phase precipitates were observed. In addition, banding characteristics of the structure are observed in Hardox 600 steel (**Fig. 3b**).

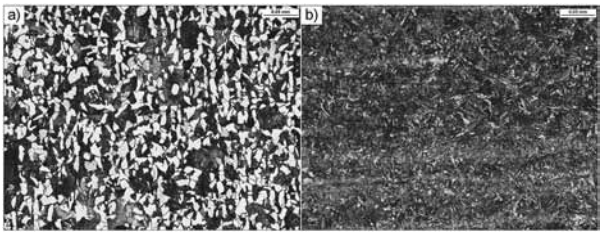

Fig. 3. Microstructures of tested steels in an as-delivered condition: (a) 38GSA (38MnSi4) steel; (b) Hardox 600 steel. Etched with 2% HNO_3; Light microscopy

Rys. 3. Mikrostruktury badanych stali w stanie dostarczenia: a) stal 38GSA (38MnSi4); b) stal Hardox 600. Trawiono 2% HNO_3; Mikroskopia świetlna

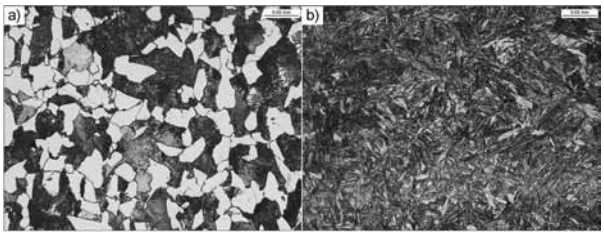

Fig. 4. An enlarged image of the microstructure of tested steels shown in Fig. 3: (a) 38GSA (38MnSi4) steel; b) Hardox 600 steel. Etched with 2% HNO_3; Light microscopy

Rys. 4. Powiększony obraz mikrostruktury badanych stali pokazanych na **Rys. 3**: a) stal 38GSA (38MnSi4); b) stal Hardox 600. Trawiono 2% HNO_3; Mikroskopia świetlna

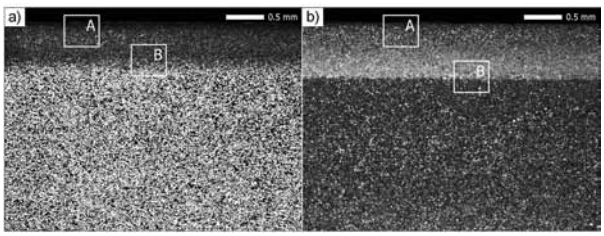

Fig. 5. Microstructures of representative samples of tested steels following laser hardening: (a) 38GSA (38MnSi4) steel; b) Hardox 600 steel. Etched with 2% HNO_3; Light microscopy

Rys. 5. Mikrostruktury reprezentatywnych próbek badanych stali po hartowaniu laserem: a) stal 38GSA (38MnSi4); b) stal Hardox 600. Trawiono 2% HNO_3; Mikroskopia świetlna

After the laser hardening operation, in the near-surface layer (Frame A in **Fig. 5**), microstructures of both tested steels were very similar to each other (**Figs. 5–7)**. Within this zone, they had a martensitic structure of varying morphology, resulting from the carbon content of these steels. The hardness distributions (**Fig. 8**) indicate that 38GSA (38MnSi4) steel reached a higher hardness level of 550-570 HV0.5 in the surface hardening process than that of Hardox 600 steel. As regards to Hardox steel, the recorded hardness ranged

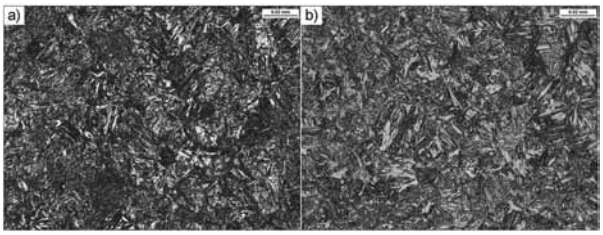

Fig. 6. Enlarged images of the microstructures of tested steels marked with frames A in Fig. 5: (a) 38GSA (38MnSi4) steel; b) Hardox 600 steel. Etched with 2% HNO_3; Light microscopy

Rys. 6. Powiększone obrazy mikrostruktur badanych stali zaznaczonych ramkami A na **Rys. 5**: stal 38GSA (38MnSi4); b) stal Hardox 600. Trawiono 2% HNO_3; Mikroskopia świetlna

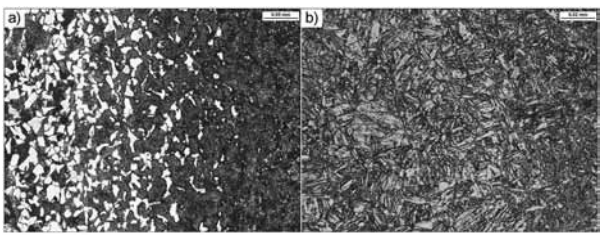

Fig. 7. Enlarged images of the microstructures of tested steels marked with frames B in Fig. 5: (a) 38GSA (38MnSi4) steel; b) Hardox 600 steel. Etched with 2% HNO_3; Light microscopy

Rys. 7. Powiększone obrazy mikrostruktur badanych stali zaznaczonych ramkami B na **Rys. 5**: stal 38GSA (38MnSi4); b) stal Hardox 600. Trawiono 2% HNO_3; Mikroskopia świetlna

from 450 to 510 HV0.5. Such significant differences in hardness in the near-surface layer of both steel grades may result from an increased silicon content of 38GSA (38MnSi4) steel, which has an advantageous effect on an increase in resistance to tempering processes as well as the prevention of irreversible tempering brittleness. On the other hand, very significant differences in the structure following laser hardening of 38GSA (38MnSi4) and Hardox 600 steel can be indicated in relation to the transition zone between the hardened layer and the native material (Frame B in **Fig. 5**). As regards to 38GSA (38MnSi4) steel, the occurrence of a widely varying microstructure comprising martensite and quenching troostite colonies as well as ferrite areas can be observed in the transition zone (**Fig. 7a**). Hardox 600 steel in the transition zone is characterised by a structure of hardening martensite with temper sorbite (**Fig. 7b**). Such morphology of the structure indicates that the laser hardening process led to processes of structure degradation resulting from the as-delivered condition of this steel (martensitic structure). Therefore, it can be concluded that, for Hardox 600 steel, all additional heat treatments should be carried out with account taken of its structure in an as-delivered condition (hardening and low-temperature tempering). Incorrect selection of heat treatment parameters (austenitising temperature

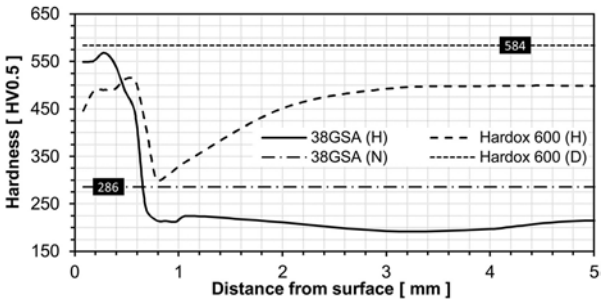

Fig. 8. Distribution of hardness of 38GSA (38MnSi4) and Hardox 600 steel samples following the laser hardening operation: N – standardised condition, D – as-delivered condition, H – laser-hardened condition

Rys. 8. Rozkłady twardości próbek stali 38GSA (38MnSi4) i Hardox 600 po operacji hartowania laserem: N – stan normalizowany, D – stan dostarczenia, H – stan zahartowany laserem

and cooling rate) may lead, in this steel, to a significant reduction in hardness level in relation to the as-delivered condition, and thus to a reduction in the abrasive wear resistance index.

Table 4 and **Figs. 9** and **10** show the results of tests for abrasive wear resistance of the analysed steels. The obtained test results indicate that Hardox 600 steel in an as-delivered condition is the most resistant to the impact of an abrasive soil mass (the smallest weight loss). The advantage of this steel over other materials applied to both types of soil, i.e. light soil (loamy sand) and heavy soil (common loam). In the light soil, an average loss of weight for Hardox 600 steel in an as-delivered condition over a friction distance of 20,000 m was smaller, compared to standardised and hardened 38GSA (38MnSi4) steel and hardened Hardox 600 steel, by, respectively, ≈1.74 g, ≈0.74 g, and ≈0.66 g. For the heavy soil, the above relationships were at the following

Table 4. A comparison of mass wear of samples of 38GSA (38MnSi4) steel and Hardox 600 steel over a friction distance of 20,000 in various types of abrasive soil masses: N – standardised condition, D – as-delivered condition, H – laser-hardened condition

Tabela 4. Zestawienie zużycia masowego próbek stali 38GSA (38MnSi4) oraz stali Hardox 600 na drodze tarcia 20000 m w różnych rodzajach glebowych mas ściernych: N – stan normalizowany, D – stan dostarczenia, H – stan zahartowany laserem

Soil mass type	38GSA (N)		38GSA (H)		HARDOX 600 (D)		HARDOX 600 (H)	
	Weight loss: AV – average value [g]; UN – unit value [g/km/cm^2]							
	AV	UN	AV	UN	AV	UN	AV	UN
LIGHT	2.4049	0.0160	1.4081	0.0094	0.6667	0.0044	1.3240	0.0088
HEAVY	3.7087	0.0247	2.0181	0.0135	0.9456	0.0063	2.5338	0.0169

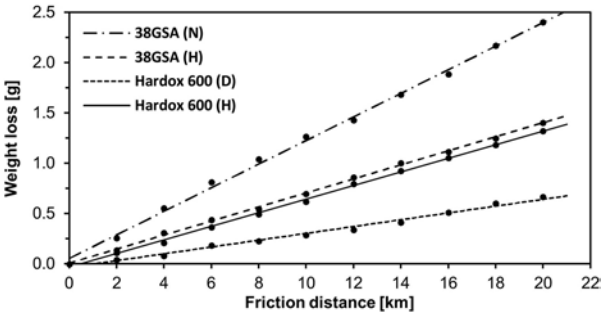

Fig. 9. The course of weight loss for the samples of tested steel as a function of the friction distance. Tests conducted in alight soil mass: N – standardised condition, D – as-delivered condition, H – laser-hardened condition

Rys. 9. Przebieg ubytku masy próbek badanych stali w funkcji drogi tarcia. Próby zrealizowane w masie glebowej lekkiej: N – stan normalizowany, D – stan dostarczenia, H – stan zahartowany laserem

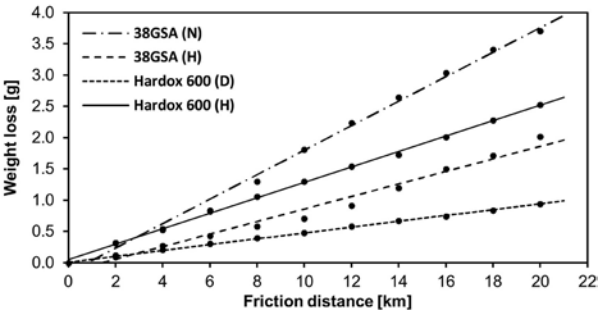

Fig. 10. The course of weight loss for the samples of tested steel as a function of the friction distance. Tests conducted in a heavy soil mass: N – standardised condition, D – as-delivered condition, H – laser-hardened condition

Rys. 10. Przebieg ubytku masy próbek badanych stali w funkcji drogi tarcia. Próby zrealizowane w masie glebowej ciężkiej: N – stan normalizowany, D – stan dostarczenia, H – stan zahartowany laserem

levels, respectively, ≈2.76 g, ≈1.07 g, and ≈1.59 g. It should also be noted that the performance of the laser surface hardening process resulted in a considerable increase in resistance to abrasive wear only for 38GSA (38MnSi4) steel. As regards to Hardox steel, the hardening treatment significantly reduced the abrasive wear resistance index compared to the as-delivered condition of the steel.

SUMMARY

In terms of resistance to abrasive wear, it can be concluded that, in both types of soil, Hardox 600 steel in an as-delivered condition was characterised by the smallest loss of weight. On the other hand, the performed laser hardening process resulted in an increase in resistance to abrasive wear only for 38GSA (38MnSi4) steel. It amounted to 70% for wear in the light soil, and to 83% in the heavy soil. As regards to Hardox 600 steel, the hardening treatment dramatically reduced the abrasive wear resistance index compared to an as-delivered condition. The main reason for such a situation may be the considerable susceptibility of this steel to tempering processes occurring during the performance of subsequent beads with a laser beam.

Spectral chemical analyses of compositions of 38GSA (38MnSi4) and Hardox 600 steels indicated lower contents of selected alloying elements in relation to the values provided in material issue lists for these steels. This is mainly the case for Hardox steel, for which only maximum values are provided. In addition, in the tested steels, the presence of chemical elements that are not mentioned in information materials for these steels was found. However, it should be stressed that the chemical composition of Hardox 600 steel is not a criterion of its classification and is only provided for information purposes.

Structural tests indicated that 38GSA (38MnSi4) steel in a standardised condition was characterised by a fine-grained ferrite-pearlite structure. This type of structure resulted in a hardness level for this steel amounting to 272 HBW. Hardox 600 steel in an as-delivered condition was characterised by a structure comprising martensite with strip morphology and few carbide phase precipitates. This type of structure indicates that this steel is only supplied by the producer in a hardened condition (without tempering processes).

The laser hardening process in the near-surface layer resulted, in both tested steels, to a very similar structure. It comprised martensite of varying morphology with hardnesses for 38GSA (38MnSi4) and Hardox 600 steel, respectively, being 550-570 HV0.5 and 450-510 HV0.5.

REFERENCES

1. Białobrzeska B., Kostencki P.: Abrasive wear characteristics of selected low-alloy boron steels as measured in both field experiments and laboratory tests, Wear 328–329 (2015) 149–159.
2. Napiórkowski J., Konat Ł., Kołakowski K.: Resistance to wear as a function of the microstructure and selected mechanical properties of microalloyed steel with boron. Tribologia 4/2016, 101–114.
3. Napiórkowski J., Konat Ł., Ligier K.: The structural properties and resistance to abrasive wear in soil of Creusabro steel. Tribologia 5/2016, 105–119.
4. Lemecha M., Napiórkowski J., Konat Ł.: Analysis of wear and tear of working elements with a replaceable cutting edge in an abrasive sill mass, Tribologia 302017,101–109.
5. Pertek-Owsiana A., Kapcińska-Popowska D., Bartkowska A.: Obróbka cieplna objętościowa i powierzchniowa stali z mikrododatkiem boru, Inżynieria Materiałowa nr 5/2014, 401–404.
6. https://www.ssab.pl/produkty/marki/hardox/products/hardox-600?accordion=downloads.
7. Jędrusik A., Kupiec B., Koronievskyi M.: Sprawność cieplna procesu spawania przy użyciu lasera cienkich blach ze stopu Inconel 718. Conference materials, International Scientific Conference: „Klaster – Odlewnictwo – Przyszłość", 09–12.09.2014.
8. BN-85/0642-48.
9. Konat Ł., Białobrzeska B., Białek P.: Effect of welding process on microstructural and mechanical characteristics of Hardox 600 steel. Metals, vol. 7, No 9, pp. 1–18, 2017.